Biochimica et Biophysica Acta 1811 (2011) 1038–1044

Contents lists available at SciVerse ScienceDirect

Biochimica et Biophysica Acta

journal homepage: www.elsevier.com/locate/bbalip

Cholesterol and membrane phospholipid compositions modulate the leakage capacity of the swaposin domain from a potato aspartic protease (*St*Asp-PSI)

Fernando Muñoz [a], M. Francisca Palomares-Jerez [b], Gustavo Daleo [a], José Villalaín [b,1], M. Gabriela Guevara [a,*,1]

[a] *Plant Biochemistry Laboratory, Biological Research Institute, National Scientific and Technical Research Council, University of Mar del Plata, Mar del Plata 7600, Argentina*
[b] *Instituto de Biología Molecular y Celular, Universidad Miguel Hernández. E-03202 Elche-Alicante, Spain*

ARTICLE INFO

Article history:
Received 7 March 2011
Received in revised form 8 July 2011
Accepted 3 August 2011
Available online xxxx

Keywords:
Antimicrobial protein
Antitumor protein
Plant aspartic protease
Membrane destabilization
α-helix protein
Plat defense response

ABSTRACT

Potato aspartic proteases (*St*APs) and their swaposin domain (*St*Asp-PSI) are proteins with cytotoxic activity which involves plasma membrane destabilization. The ability of these proteins to produce cell death varies with the cellular type. Therefore, *St*APs and *St*Asp-PSI selective cytotoxicity could be attributed to the different membrane lipid compositions of target cells. In this work we investigate the possible mechanism by which *St*APs and *St*Asp-PSI produce selective membrane destabilization. Results obtained from leakage assays show that *St*Asp-PSI is a potent inducer of the leakage of LUVs containing anionic phospholipids, especially those containing phosphatidylglycerol. Based in these results, we suggest that the cytotoxic activity of *St*Asp-PSI on pathogenic microorganisms could be mediated by the attraction between the exposed positive domains of *St*Asp-PSI and the negatively charged microorganism membrane. On the other hand, our circular dichroism spectroscopic measurements and analysis by size exclusion chromatography and followed by electrophoresis, indicate that hydrophobic environment is necessary to *St*Asp-PSI oligomerization and both *St*Asp-PSI disulfide bounds and membrane with negative charged phospholipids are required by *St*Asp-PSI to produce membrane destabilization and then induce cell death in tumors and microorganism cell targets. Additionally, we demonstrate that the presence of cholesterol into the LUV membranes strongly diminishes the capacity of *St*Asp-PSI to produce leakage. This result suggests that the lack of hemolytic and cytotoxic activities on human lymphocytes of *St*Asp-PSI/*St*APs may be partly due by the presence of cholesterol in these cell membrane types.

1. Introduction

Aspartic proteases (EC 3.4.23) (AP) are a class of widely distributed proteases present in animals, microbes, viruses and plants [1,2]. Biological functions of plant APs have not yet been characterized to the extent of their mammalian, microbial or viral counterparts [1–4]. Most of plant AP sequences predict preproproteins, as in the case of animal and fungal aspartic proteases, with a signal peptide and a proregion at the amino-terminus of the mature protein [5]. However, plant AP genes have an extra region of approximately 100 amino acids known as "plant specific insert" (PSI) [3,4], similar to saposin-*like* proteins (SAPLIP) (Fig. 1A). Structural analysis of PSI domains reveals a compact globular structure formed by 5 alpha-helices linked to each other by disulfide bridges [4,6]. PSI is not a true saposin domain; it is the swap of the N- and C-terminal portions of the saposin like domain; hence, PSI is named as swaposin domain [4] (Fig. 1B).

Saposin and saposin-*like* proteins and domains have diverse *in vivo* biological functions or are implicated in different physiological functions [7]. All these proteins bind to or interact with lipid membranes and its "saposin-fold" is a common fold in a single globular structure [6–12] (Fig. 1C). Despite the conserved structural organization of SAPLIPs, their distinct modes of interaction with biological membranes are not fully understood. This could be the result of the differential interactions with the biological membrane environments and/or differences in lipid cell membrane composition [12–16]. Several functions have been proposed for PSI domain, as the targeting to the vacuole; vesicle leakage and a role in the processing of the mature enzyme [4,14,17]; however, their role(s) in the plants is/are still speculative.

Previously, we have reported the cloned, heterologous expression and purification of the PSI domain from a *Solanum tuberosum* aspartic protease (*St*Asp-PSI) [6]. *St*Asp-PSI has high structural similarity with

Abbreviations: AP, aspartic proteases; CD, circular dichroism; CF, 5-Carboxyfluorescein; Chol, Cholesterol; DTT, dithiothreitol; EPA, egg phosphatidic acid; EPC, egg L-α-phosphatidylcholine; EPG, egg L-α-phosphatidylglycerol; LUV, large unilamellar vesicles; MLV, multilamellar vesicles; PCD, programmed cell death; PSI, plant specific insert; SAPLIP, saposin-like proteins; *St*AP, *Solanum tuberosum* aspartic proteases; SUV, small unilamellar vesicles; TFE, 2,2,2-trifluoroethanol; TPE, egg trans-esterified L-α-phosphatidylethanolamine

* Corresponding author at: 3250 Funes, 4th Floor, Mar del Plata 7600, Argentina. Tel.: +54 223 4753030x14; fax: +54 223 4724143.
E-mail address: gguevara@mdp.edu.ar (M.G. Guevara).

[1] Equal contribution.

1388-1981/$ – see front matter © 2011 Elsevier B.V. All rights reserved.
doi:10.1016/j.bbalip.2011.08.013

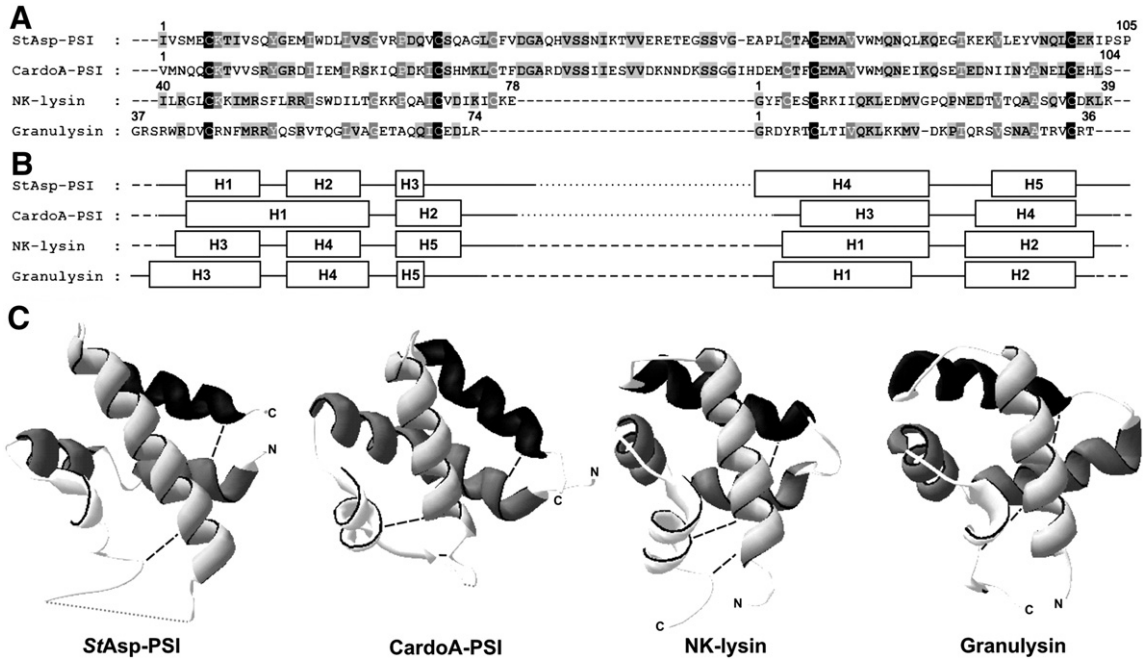

Fig. 1. Sequence and structural homology between *St*Asp-PSI, CardoA-PSI and SAPLIPs. (A) Amino acid sequence alignment of the PSI domain of *St*Asp-PSI (GeneBank accession no. AY672651) and CardoAPSI (GeneBank accession no. AJ132884) and permuted sequences of NK-lysin (GeneBank accession no. Q29075) and Granulysin (GeneBank accession no. EAW99485). Sequences retrieved from databases were automatically aligned using CLUSTAL W algorithm. Conserved cysteines are highlighted in black, identical residues are highlighted in gray and gaps are indicated by dashes. (B) The α-helical regions are indicated by boxes. The disordered part of the PSIs is marked by dotted line and gaps are indicated by dashes. (**C**) Ribbon representation of the model structure of the PSI domain of *St*Asp-PSI and CardoAPSI based on the crystal structure of prophytepsin-PSI (PDB accession no. 1QDM) and crystal structures of NK-lysin and Granulysin. Similar helixes are displayed in same color. The disordered part of the PSIs is marked by dotted line and disulfide bridges by dashed lines. Similarities between *St*Asp-PSI, CardoAPSI, NK-lysin (PDB: 1NKL) and Granulysin (PDB: 1L9L) were determined using DeepView/Swiss-PdbViewer 3.7 program.

two saposin-*like* proteins with antimicrobial activity, NK-lysin and granulysin [6,7]. Like these SAPLIPs, the *St*Asp-PSI domain is able to interact with cell plasma membranes, increasing the cell permeability and finally, producing cell death [6,18]. Additionally, in previous reports we demonstrated that the cytotoxic activity of *St*APs and *St*Asp-PSI is selective. Whereas these proteins are toxic to plant and human pathogen microorganisms and cancer cells, they are not able to kill human T cells, human red blood cells and plant cells [6,18–23]. Like with a vast number of antimicrobial peptides from various sources, *St*APs and *St*Asp-PSI have been isolated and characterized; however, the molecular explanation for their target specificity, or conversely, the reason of the different susceptibilities of cells from different origins to these proteins is not yet understood [6,18–24].

In order to search for the possible reasons of the differential cytotoxic activity of *St*Asp-PSI and *St*APs, we have analyzed in this work the ability of *St*Asp-PSI to induce membrane rupture of LUVs with different phospholipid compositions as well as changes in the *St*Asp-PSI secondary structure and oligomerization capacity in membrane like environments.

2. Materials and methods

2.1. Protein expression and purification

Recombinant *St*Asp-PSI was overexpressed in *Escherichia coli* M15 and purified as described previously [6]. Protein was stored in 50 mM phosphate buffer, 25 mM NaCl, pH 7. Protein concentration was measured by the bicinchoninic acid method [25], using BSA as the standard.

2.2. Materials and reagents

Cholesterol (Chol), total bovine liver lipid extract (liver extract), egg phosphatidic acid (EPA), egg L-α-phosphatidylcholine (EPC), egg L-α-phosphatidylglycerol (EPG), and egg trans-esterified L-α-phosphatidylethanolamine (TPE) were obtained from Avanti Polar Lipids (Alabaster, AL, USA). Calcein, 5-Carboxyfluorescein (CF, >95% by HPLC), dithiothreitol (DTT), 2,2,2-trifluoroethanol (TFE), Triton X-100 and EDTA were purchased from Sigma-Aldrich (Madrid, ES). All other chemicals were commercial samples of the highest purity available (Sigma-Aldrich, Madrid, ES). Water was deionized, twice-distilled and passed through a Milli-Q equipment (Millipore Ibérica, Madrid, ES) to a resistivity higher than 18 MΩ cm.

2.3. Vesicle preparation

Aliquots containing the appropriate amount of lipid in chloroform-methanol (2:1 vol/vol) were placed in a test tube, the solvents were removed by evaporation under stream of O_2-free nitrogen, and finally, traces of solvents were eliminated under vacuum in the dark for>3 h. The lipid films were resuspended in an appropriate buffer and incubated either at 25 °C or 10 °C above the phase transition temperature (T_m) with intermittent vortexing for 30 min to hydrate the samples and obtain multilamellar vesicles (MLV). The samples were frozen and thawed five times to ensure complete homogenization and maximization of protein/lipid contacts with occasional vortexing. Large unilamellar vesicles (LUV) with a mean diameter of 0.1 μm were prepared from MLV by the extrusion method [26] using polycarbonate filters with a pore size of 0.1 μm (Nucleopore Corp., Cambridge, CA, USA). Small unilamellar vesicles (SUV) were prepared from MLVs using a Branson 250 sonifier (40 W) equipped with a microtip until the suspension became completely transparent. Every 30 s, the samples were cooled for 90 s in ice to prevent overheating of the solution. The titanium particles from the tip were removed by centrifugation at 15000 rpm at room temperature for 15 min. For circular dichroism (CD) spectroscopy, SUVs of different lipid composition were mixed with *St*Asp-PSI to a protein/lipid ratio 1:25. The phospholipid concentration was measured as described previously [27].

2.4. Membrane leakage measurement

For assays of vesicle leakage at pH 7, LUVs with a mean diameter of 0.1 μm were prepared as indicated above in buffer containing 10 mM Tris–HCl, 20 mM NaCl, 40 mM CF, and 0.1 mM EDTA, pH 7 [28], whereas for assays of vesicle leakage at pH 5.4, in buffer containing 20 mM citrate, 20 mM NaCl, and 40 mM calcein, pH 5.4 [29]. Breakdown of the vesicle membrane leads to content leakage, i.e., CF or calcein fluorescence. Nonencapsulated CF or calcein was separated from the vesicle suspension through a Sephadex G-75 filtration column (Pharmacia, Uppsala, Sweden) eluted with buffer containing either 10 mM Tris–HCl, 100 mM NaCl, and 0.1 mM EDTA, pH 7, or 20 mM citrate, 100 mM NaCl, and 0.1 mM EDTA, pH 5.4. Leakage of intraliposomal CF or calcein was assayed by treating the probe-loaded liposomes (final lipid concentration, 0.125 mM) with the appropriate amounts of *St*Asp-PSI on microtiter plates stabilized at 25 °C using a microplate reader (FLUOstar, BMG Labtech, Germany), each well containing a final volume of 170 μl. The medium in the microtiter plates was continuously stirred to allow the rapid mixing of *St*Asp-PSI and vesicles. One hundred percent release was achieved by adding Triton X-100 to the microtiter plate to final concentration of 0.5% (w/w). Changes in fluorescence intensity were recorded with excitation and emission wavelengths set at 492 and 517 nm, respectively. Excitation and emission slits were set at 5 nm. Leakage was quantified on a percentage basis as previously described [30,31].

2.5. Circular dichroism (CD) spectroscopy

Circular dichroism spectra were collected on a Jasco J810 spectropolarimeter fitted with a thermostated cell holder and interfaced with a Neslab RTE-111 water bath. Spectral scans were performed from 250 to 195 nm at 25 °C, with step resolution of 0.2 nm and bandwidth of 2 nm. The counting rate was 50 nm/min with 2 s response time. A 1 mm path length quartz cuvette was used for the measurements, values from 10 scans were averaged per sample to improve the signal-to-noise ratio and corrected for the contributions of vesicles and buffer. Subtracted spectra were smoothed avoiding alteration of spectral intensities. SUVs were used to obtain CD spectra. No changes in turbidity (as measured at 445 nm) were observed after *St*Asp-PSI addition to the SUV solutions. The results are expressed as a mean of the residue ellipticity, [θ], using a value of 93.96 g/mol for the molecular weight of the mean residue. Secondary structure fractions (α-helix, β-sheet and random coil) were determined by the use of the K2D2 web server accessible at http://www.ogic.ca/projects/k2d2/ [32]. The estimated maximum error used for the prediction analysis was 0.4.

2.6. Size exclusion chromatography

Oligomeric state of *St*Asp-PSI in the absence or presence of 15% TFE was estimated by size exclusion chromatography on an equilibrated Superdex 75 HR (10/30) column (Pharmacia, Uppsala, Sweden), connected to a fast-protein liquid chromatography system, at a constant flow rate of 1 ml/min at room temperature. The column was calibrated using a mixture of four proteins of known molecular mass, i.e. ovalbumin (44.3 kDa), glyceraldehyde-3P-dehydrogenase (36 kDa), lysozyme (14.3 kDa), and insulin (6 kDa). The column was equilibrated with 50 mM phosphate buffer, 25 mM NaCl, pH 7, with or without 15% TFE. Samples with TFE were incubated for 2 h at 37 °C before load into the column. Fractions of 1 ml were collected and the elution was monitored at 280 nm.

2.7. Gel electrophoresis

The complex formation of *St*Asp-PSI in presence of 15% TFE was investigated by NATIVE-PAGE analysis using 15% (w/v) acrylamide gel, according to [33] and a running buffer containing 96 mM glycine and 12.5 mM Tris, pH 8.8. Samples with TFE were incubated for 2 h at 37 °C before NATIVE-PAGE was made. Gels were stained with silver nitrate as described previously [34].

3. Results

3.1. StAsp-PSI permeabilizes negatively charged membranes

In order to analyze the interaction of *St*Asp-PSI with phospholipid membranes, artificial vesicles consisting of lipids only were used. We tested the ability of *St*Asp-PSI to rupture membrane vesicles by monitoring the release of fluorescent probes trapped inside the liposomes. We evaluated also the effect of the different phospholipid composition on the capability of *St*Asp-PSI to interact with membranes. The different phospholipids used in this work were the negatively charged lipids EPG and EPA and the zwitterionic lipids EPC and TPE. Vesicles containing cholesterol and lipids from a liver extract were used to study the effect of *St*Asp-PSI on membranes resembling mammalian plasma membranes.

Fig. 2 shows the capability of *St*Asp-PSI to induce CF release from preloaded LUVs. Furthermore, the extent of release was dependent on the LUV phospholipid composition. The results obtained show that *St*Asp-PSI was able to produce vesicle leakage and the release of vesicle content of LUVs containing negative phospholipids in a dose-dependent manner (Fig. 2). In contrast, *St*Asp-PSI was unable to permeabilize LUVs composed of zwitterionic phospholipids (EPC and TPE) or a liver lipid extract, at the different times and *St*Asp-PSI concentrations assayed. In LUVs containing EPC/EPA and EPC/EPG at molar ratios of 5:4, 50% of the vesicle contents were released at 3.5 μM and 2.25 μM of *St*Asp-PSI, respectively. The importance of the disulfide bonds in the capability of *St*Asp-PSI to permeabilize LUVs was clearly observed when this protein was preincubated with DTT. As it can be observed in Fig. 2, reduced *St*Asp-PSI was not able to induce the CF release from vesicles at any times, protein amounts and LUV compositions assayed.

The leakage of LUVs induced by *St*Asp-PSI was found to be pH-dependent (Fig. 3). In EPC/EPG containing vesicles, the initial rate and the maximal percentage of the fluorescence release induced by *St*Asp-PSI were dose-dependent at pH 7 (Fig. 3A). The highest percentage of CF release was observed at 8.3 μM *St*Asp-PSI (about 85%) at pH 7, whereas at pH 5.4 only 50% of the trapped calcein was released with this *St*Asp-PSI concentration.

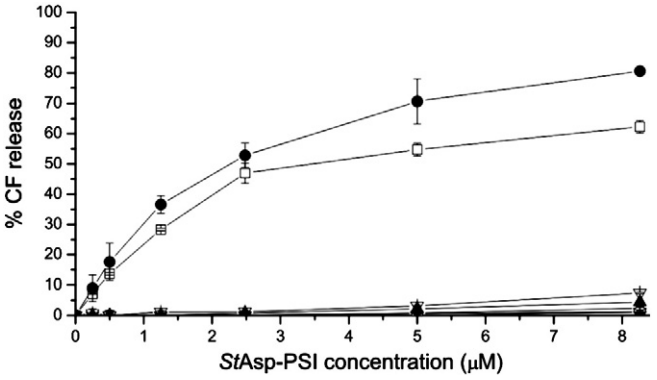

Fig. 2. Effect of *St*Asp-PSI on the release of LUV contents for different lipid compositions at pH 7 and 45 min of incubation. The lipid compositions used were EPC (○), EPC/TPE at a molar ratio of 5:2 (▼), EPC/EPG at a molar ratio of 5:4 (●), EPC/EPA at a molar ratio 5:4 (□), EPC/Chol at a molar ratio 5:2 (■), liver extract (△), EPC/EPG at a molar ratio 5:4 in the presence of 0.2 mM DTT (▲), and EPC/EPA at a molar ratio of 5:4 in the presence of 0.2 mM DTT ( ). Error bars indicate standard deviations of the mean of triplicate samples.

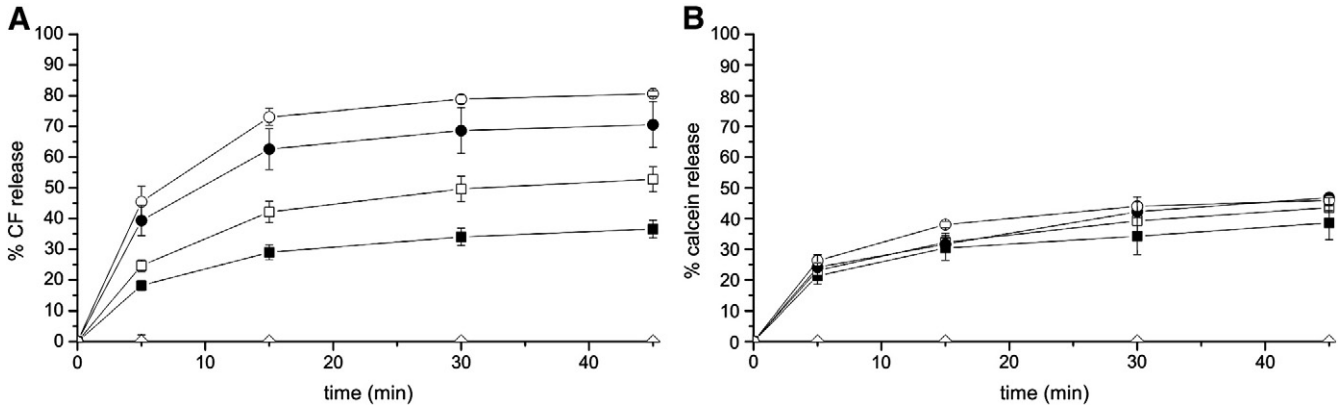

Fig. 3. Effect of *St*Asp-PSI on the release of LUV contents from membranes composed of EPC/EPG at a molar ratio of 5:4 at pH 7 (A) and pH 5.4 (B). The *St*Asp-PSI concentrations used were 0 μM (◊), 1.25 μM (■), 2.48 μM (□), 5 μM (●), and 8.26 μM (○). Error bars indicate standard deviations of the mean of triplicate samples.

3.2. Cholesterol affects the StAsp-PSI leakage activity

We tested the ability of *St*Asp-PSI to produce leakage on vesicles with eukaryote membrane like composition (liver extract-containing vesicles and cholesterol-containing vesicles). Fig. 2 shows that *St*Asp-PSI was unable to permeabilize membranes of LUVs containing the complex liver lipids mixture at all *St*Asp-PSI concentration and times assayed.

Results observed in Fig. 4 show that the presence of cholesterol reduces the CF release produced by *St*Asp-PSI in both EPC/EPA and EPC/EPG containing vesicles. In EPC/EPA/Chol containing vesicles the cholesterol effect is dose-dependent at all *St*Asp-PSI amounts assayed (Fig. 4A). However, in EPC/EPG/Chol containing vesicles this effect was more evident and stronger; at a lipid molar ratio 5:4:1, the leakage produced by *St*Asp-PSI diminishes in a 90% approximately (Fig. 4B).

3.3. Secondary structure of StAsp-PSI

The far-UV CD spectra (195–250 nm) of *St*Asp-PSI domain in 50 mM phosphate buffer pH 7 at 25 °C shows two strong ellipticity values around 208 and 222 nm that indicate the presence of helical conformations (Fig. 5). Analysis of the solution CD spectra of *St*Asp-PSI using the K2D2 method [32] also suggested that the protein had a dominant helical conformation (54%) (Table 1) with lesser contributions from β-sheet components (6%) and random structures (40%).

In order to evaluate the effect of lipid membrane composition on the *St*Asp-PSI secondary structure we determined whether its CD spectrum changed in presence of SUVs containing zwitterionic lipids (EPC); zwitterionic and negative lipids (EPC/EPA; EPC/EPG) (Fig. 5A). Data showed in Table 1 demonstrate that, in SUVs containing EPC, a decrease of *St*Asp-PSI α-helix content from was observed (from 54% to 48%). When *St*Asp-PSI was incubated with SUVs containing negatively charged phospholipids, a significant decrease in the α-helix content was observed, from 54% to 32% and 27% for SUVs containing EPC/EPA and EPC/EPG at molar ratios of 5:2, respectively. No significant changes were observed in the *St*Asp-PSI secondary structure in the presence of DTT (Fig. 5B).

The ratio of the ellipticities at 222 and 208 nm can be utilized to distinguish between monomeric and oligomeric states of helices [35]; when the ratio $\theta_{222}/\theta_{208}$ is about 0.8, the peptide is in its monomeric state, and when the ratio exceeds the value of 1.0 is in the oligomeric state. Results obtained show that in presence of SUVs containing EPC the *St*Asp-PSI ratio $\theta_{222}/\theta_{208}$ is 0.8, suggesting that *St*Asp-PSI is mainly in the monomeric state. In the presence of SUVs containing EPC/EPA and EPC/EPG at molar ratios of 5:2, the *St*Asp-PSI $\theta_{222}/\theta_{208}$ ratios were approximately 1.9 and 1.5 respectively. These values suggest that in the presence of SUVs containing negatively-charged phospholipids, *St*Asp-PSI is mostly in oligomeric state.

To study the tendency of *St*Asp-PSI to oligomerize we performed size exclusion chromatography in presence of trifluoroethanol (TFE) as described in the materials and methods section. TFE is one of the most frequently used membrane-mimetic organic co-solvents to determine the

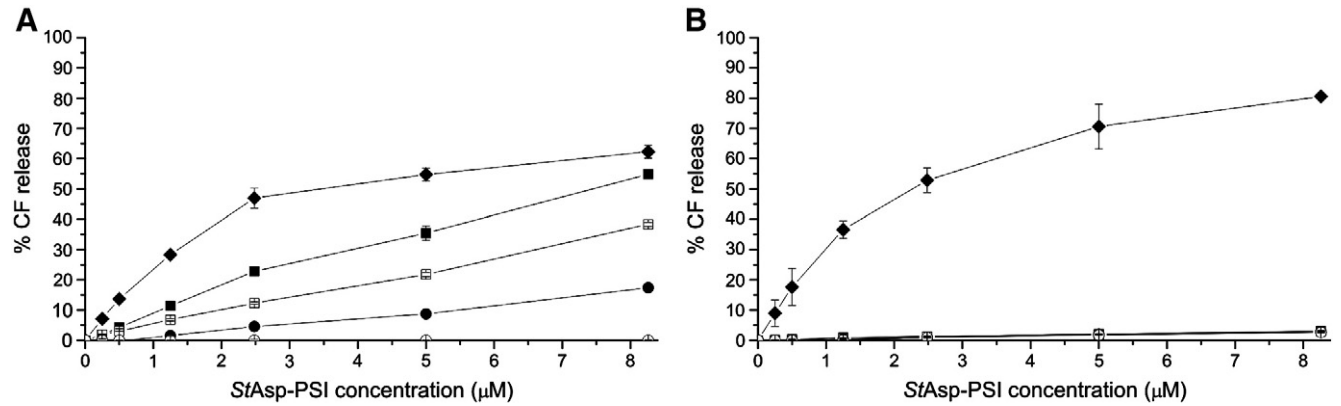

Fig. 4. Effect of Chol on *St*Asp-PSI-induced release of LUV contents on negatively charged membranes containing either EPA (A) or EPG (B) at pH 7 and 45 min of incubation. Lipid compositions containing EPA (A) were EPC/EPA at a molar ratio of 5:4 (♦), EPC/EPA/Chol at a molar ratio of 5:4:1 (■), EPC/EPA/Chol at a molar ratio of 5:4:2 (□), EPC/EPA/Chol at a molar ratio of 5:4:3 (●), and EPC/EPA/Chol at a molar ratio of 5:4:4 (○). Lipid compositions containing EPG (B) were EPC/EPG at a molar ratio of 5:4 (♦), EPC/EPG/Chol at a molar ratio of 5:4:1 (■), EPC/EPG/Chol at a molar ratio of 5:4:2 (□), EPC/EPG/Chol at a molar ratio of 5:4:3 (●), and EPC/EPG/Chol at a molar ratio of 5:4:4 (○). Error bars indicate standard deviations of the mean of triplicate samples.

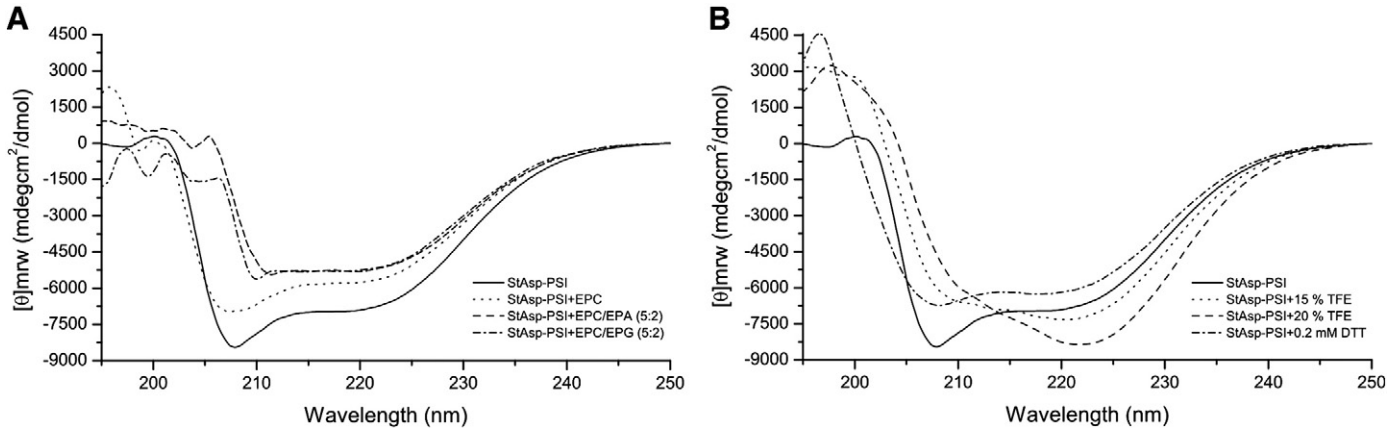

Fig. 5. CD spectra of *St*Asp-PSI in solution, bound to SUVs containing different phospholipidic compositions (**A**) and in the presence of different TFE concentrations or 0.2 mM DTT (B), at pH 7 and 25 ºC. Protein concentration was 50 μM for all the samples, and the lipid/protein ratio was 25:1. *[θ]mrw*, mean of the residue ellipticity.

induced conformation relevant to peptide antimicrobial activity [36,37]. When proteins or peptides are transferred from water to membrane like interfaces, a decrease in the proteins or peptides environmental polarity occurs. The data obtained show that no significant changes were detected in the *St*Asp-PSI α-helix content in the presence of 15% and 20% TFE (Fig. 5B, Table 1). At 15% TFE, *St*Asp-PSI adopts an α-helical conformation with the monomer/oligomer equilibrium shifted toward the oligomeric state with a ratio $\theta_{222}/\theta_{208}$ of approximately 1.2, and at 20% TFE the ratio increases to 1.8, showing that the predominant state is the oligomeric one.

*St*Asp-PSI was chromatographed in a size exclusion chromatography under hydrophilic and hydrophobic conditions in order to determine, by an experimental procedure, the transition of *St*Asp-PSI from the monomeric state to the oligomeric state. The chromatographic profile obtained under hydrophilic conditions shows a unique peak; corresponding to a molecular weight of 10 kDa, approximately (Fig. 6A). In the presence of 15% TFE, three peaks were determined in the column elution profile, corresponding to molecular weights of 10 kDa and 22 kDa, approximately, and another peak corresponding to a molecular weight greater than 100 kDa. The band pattern of the size exclusion chromatography pools analyzed by NATIVE-PAGE shows a unique band and three bands in hydrophilic and hydrophobic conditions respectively (Fig. 6B, lanes 1 and 2). These results are in agreement with the results predicted from the CD data, and support the fact that the *St*Asp-PSI domain is present in a monomeric form under hydrophilic conditions; however, *St*Asp-PSI has a tendency to form dimers and/or higher order oligomers in a hydrophobic environment.

Additionally, the importance of the intermolecular disulfide bonds in the *St*Asp-PSI oligomerization was demonstrated when, a decrease in the amount of the dimeric form and an increase in the amount of the monomeric form were observed in presence of 15% TFE and DTT (Fig. 6A and B, lane 3).

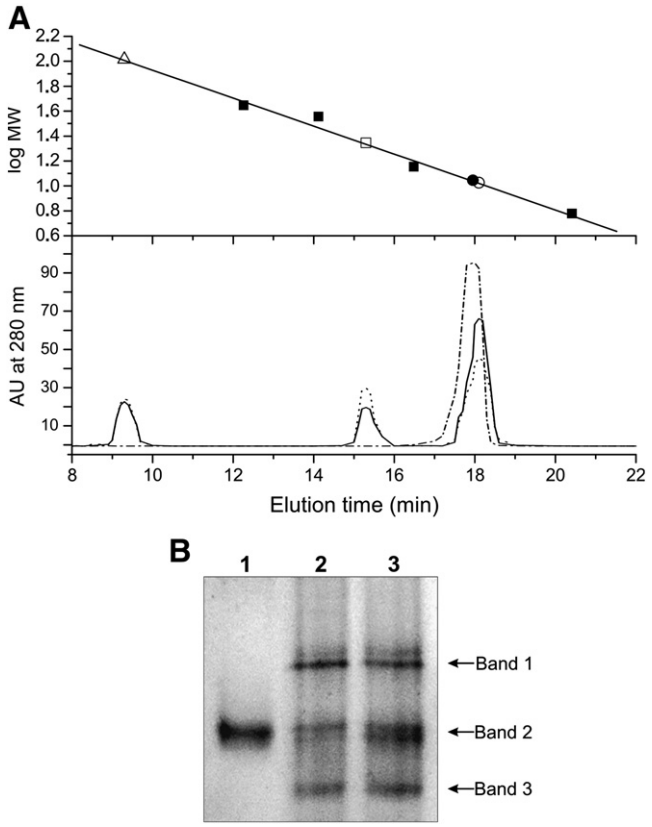

Table 1
Estimation of the secondary structure content of *St*Asp-PSI in solution with or without DTT, TFE, and bound to SUVs of different phospholipidic composition at pH 7 and 25 °C, as determined by circular dichroism using the K2D2 algorithm. Conformation values have been rounded to the next integer.

	α-helix	β-sheet	Random coil	$\theta_{222}/\theta_{208}$	Protein state
*St*Asp-PSI	54	6	40	0.8	Monomeric
*St*Asp-PSI + 0.2 mM DTT	51	8	41	0.9	Monomeric
*St*Asp-PSI + 15% TFE	52	9	39	1.2	Oligomeric
*St*Asp-PSI + 20% TFE	55	8	36	1.8	Oligomeric
*St*Asp-PSI + EPC	48	8	44	0.8	Monomeric
*St*Asp-PSI + EPC/EPA (5:2)	31	14	55	1.9	Oligomeric
*St*Asp-PSI + EPC/EPG (5:2)	27	18	55	1.5	Oligomeric

Fig. 6. Oligomeric state of *St*Asp-PSI. (A) The upper panel shows the calibration curve as well as the elution times of *St*Asp-PSI in the absence or presence of 15% TFE. Elution times of proteins used for calibration are indicated by solid squares, and elution times of *St*Asp-PSI under the different conditions are indicated according to the different oligomeric state (monomeric *St*Asp-PSI without TFE (●), monomeric *St*Asp-PSI in TFE (○), dimeric *St*Asp-PSI in TFE (□), high MW *St*Asp-PSI in TFE (Δ). The lower panel contains the elution profiles of *St*Asp-PSI from Superdex 75 HR 10/30 column. Experiments were performed at pH 7 in the absence (*dashed-dotted line*), in the presence of 15% TFE (*dotted line*) or in the presence of 15% TFE, previously treated with 1 mM DTT for 3 h at 37 ºC (*solid line*). The protein elutes as a monomer in the absence of TFE, and predominantly as a monomer and dimer in the presence of TFE. Absorption (arbitrary units, AU) was measured at 280 nm. (B) NATIVE-PAGE analysis of the molecular organization of *St*Asp-PSI in the absence (*lane 1*), in the presence of TFE (*lane 2*) or previously treated with 1 mM DTT for 3 h at 37 ºC in the presence of TFE (*lane 3*). Gel was silver stained.

4. Discussion

We have previously reported that *St*APs and *St*Asp-PSI have cytotoxic activity, that this activity involves plasma membrane destabilization and that the ability of these proteins to produce cell death is dependent of the cellular type [6,18,21]. The results herein presented contribute to understand the possible selective mechanism underlying the cytotoxic activity of *St*APs and *St*Asp-PSI.

Results obtained here show that *St*Asp-PSI is a potent inducer of the leakage of LUVs containing anionic phospholipids. In agreement with the results reported for other α-helix antimicrobial peptides, *St*Asp-PSI shows a remarkable preference for phosphatidylglycerol and the inability to permeabilize LUVs containing only zwitterionic phospholipids [24]. As described for these peptides, the preference of *St*Asp-PSI to interact with LUVs with negative charge may be explained by the electrostatic interactions produced between the positives exposed protein domains and the negative charge of LUVs [38–40]. Natural cell membranes are complex entities consisting of a variety of components. Eukaryotic and prokaryotic cell membranes differ in their physical and chemical properties. Specifically, prokaryotic cell membranes contain higher amounts of anionic phospholipids than eukaryotic cell membranes, but do not contain sphingomyelin and cholesterol [41–46]. Therefore, the interaction of *St*Asp-PSI with plant and human pathogenic microorganisms and the subsequent pathogen cell death could be explained as the attraction between the exposed positive domains of *St*Asp-PSI and the negatively charged microorganism membrane.

Several reports relate the hemolytic activity of antimicrobial peptides with the capacity of these peptides to strongly interact with either membranes, containing cholesterol or not [47,48]. Like in the case of antimicrobial peptides unable to lyse red blood cells [49], the presence of cholesterol into the LUV membranes strongly diminishes the capacity of *St*Asp-PSI to produce leakage, in a dose-dependent manner and at all *St*Asp-PSI concentration assayed. Cholesterol presence in the membranes causes a reduction of the density of the hydrophobic head group at the interfacial region of the bilayer and an increase in the packaging of the phospholipid tails in the middle of the bilayer [50]. Therefore, the high rate of hydration of lipid head group at the interface bilayer region found in cholesterol-rich membranes is probably responsible to reduce the *St*Asp-PSI–LUV interaction. As reported before for other antimicrobial peptides [48], we suggest that the loss detected in the *St*Asp-PSI leakage capacity may be a consequence of a non relevant *St*Asp-PSI insertion into the bilayer and probably only a transient binding occurs that do not significantly affect the stability of the membranes of cholesterol containing LUVs. This suggestion is supported by previous results that show that *St*Asp-PSI/*St*APs are able to bind to human red blood cells, but do not produce plasma cell membrane destabilization and therefore cell death [6,18]. Thus, the lack of hemolytic and cytotoxic activities on human lymphocytes of *St*Asp-PSI/*St*APs may be partly due by the presence of cholesterol in these cell membrane types. Future assays using calorimetry, infrared and NMR should be performed to corroborate this hypothesis.

On the other hand, we have attempted to analyze the possible structural changes in *St*Asp-PSI induced by interaction with membranes differing in lipid composition. Analysis of CD data indicates that, in the presence of lipid vesicles containing negatively charged phospholipids, *St*Asp-PSI undergoes significant changes in its secondary structure. These changes consist in a decrease in the α-helix content and an increase in the percentage of random coil. Contrary to this, in the presence of vesicles containing only zwitterionic phospholipids or in the presence of TFE a non-significant change in the *St*Asp-PSI overall structure was observed. Additionally, analysis by size exclusion chromatography and electrophoresis showed that *St*Asp-PSI is a monomer in a hydrophilic environment, whereas in a hydrophobic one monomeric, dimmeric and aggregated forms are found. These results are consistent with the scheme proposed by Khandelia et al., (2008) [51] where, the secondary structure induced in different peptides ultimately determines their selectivity profile. Hence for *St*Asp-PSI, as well as for other AMPs [52–54], the membrane has as strong influence on peptide conformation as the peptide has on membrane integrity.

We have previously reported the importance of disulfide bonds in *St*Asp-PSI antitumor and antimicrobial activity [6,21]. Here, we demonstrate that the reduction of disulfide bonds does not induce significant changes in the *St*Asp-PSI secondary structure. However, as a consequence of disulfide bonds reduction *St*Asp-PSI loses its vesicle leakage capacity, and there is a transition to the monomeric *St*Asp-PSI state from the *St*Asp-PSI dimeric and oligomeric states. These data and the prediction analysis of CD assays suggest that the aggregation of *St*Asp-PSI is necessary for peptide induced vesicle leakage and cytotoxic activity on tumor and microorganism cells, like in other SAPLIPs [6,18,21]. Therefore, a hydrophobic environment is necessary to produce *St*Asp-PSI oligomerization and both, *St*Asp-PSI disulfide bonds and membrane with negatively-charged phospholipids, are required by *St*Asp-PSI to produce membrane destabilization and then induce cell death in tumors and microorganism cell targets.

Finally, and in order to correlate the results herein shown with the possible biological role of *St*Asp-PSI/*St*APs in the plant defense response, we have focused our attention to three facts. In the first place, the changes in phospholipid plasma membrane composition in plant cells under stress conditions. Several reports reveal the existence of two major phospholipid components: phosphatidylcholine and phosphatidylethanolamine; and minor components as, phosphatidylinositol, phosphatidylserine and phosphatidylglicerol into the plasma cell membranes of a great number of plant species [55,56]. On the other hand, changes in the plasma membrane phospholipids content have been reported when plants are exposed to stress conditions. In *Arabidopsis thaliana*, the content of phosphatidic acid increases while a decrease of the content of phosphatidylcholine and phosphatidylethanolamine was observed. The authors suggest that, the loss in phosphatidylcholine and the increase in phosphatidic acid content may be responsible of destabilizing membrane bilayer structure, resulting in cell death [56]. In the second place, the preference of *St*Asp-PSI to permeabilize LUVs containing phosphatidic acid, i.e., with a negative net charge, has been described above. Thirdly, the presence of the PSI domain in the amino acid sequences of plant AP precursors or mature proteins, including *St*APs; and the localization of these proteins in tissues undergoing programmed cell death (PCD) [22,23,57–59]. PSI functions in plant APs are still unclear; however, several roles have been suggested in the plant PCD [10,14,60–62]. Specifically, the presence of this domain into the mature AP proteins from potato (*St*APs); tomato (*Lyco*AP) [63] and *Nepenthes alata* (*Na*AP4) [64], has been considered as being a part of the defensive machinery against pathogens and/or an effector of cell death [14,18,64]. Therefore, this background, together with the results obtained here, allow us to suggest that destabilization of plasma membrane of stressed cells may be a consequence of changes in the chemical and physical properties of the plasma cell membranes and/or proteins that, like *St*Asp-PSI, are able to permeabilize membranes containing mainly negative phospholipids. All these events, together or separately, cause the subsequent cell death. On the basis of the antecedents and results described above, we propose that, the possible role of *St*APs as pathogenesis related proteins into the plant defensive response is to interact with the pathogen plasma membrane causing membrane destabilization and subsequently pathogen cell death and/or kill plant cells under stress conditions, contributing to circumscribe pathogen spread and colonization.

Acknowledgements

This work was supported in part by grant BFU2008-02617-BMC (Ministerio de Ciencia y Tecnología, Spain) to J.V.; National Scientific and Technical Research Council grant (CONICET) to M.G.G.; Scientific

Research Commission of the Province of Buenos Aires (CIC) grant to G.D. and University of Mar del Plata grant to G.D. and M.G.G. F.M. is fellow of CONICET; G.D. is an established researcher of CIC and M.G.G. is an established researcher of CONICET. F.M. is grateful for a fellowship (MAEC-AECI 2009–2010) of the Spanish Ministry of Foreign Affairs and Cooperation.

References

[1] D.R. Davies, The structure and function of the aspartic proteinases, Annu. Rev. Biophys. Biophys. Chem. 19 (1990) 189–215.
[2] N.D. Rawlings, A.J. Barrett, Families of aspartic peptidases, and those of unknown catalytic mechanism, Meth. Enzymol 248 (1995) 105–120.
[3] A. Mutlu, S. Gal, Plant aspartic proteinases: enzymes on the way to a function, Physiol. Plant. 105 (1999) 569–576.
[4] I. Simoes, C. Faro, Structure and function of plant aspartic proteinases, Eur. J. Biochem. 271 (11) (2004) 2067–2075.
[5] I. Simoes, et al., Characterization of recombinant CDR1, an Arabidopsis aspartic proteinase involved in disease resistance, J. Biol. Chem. 282 (43) (2007) 31358–31365.
[6] F.F. Munoz, et al., The swaposin-like domain of potato aspartic protease (StAsp-PSI) exerts antimicrobial activity on plant and human pathogens, Peptides 31 (5) (2010) 777–785.
[7] H. Bruhn, A short guided tour through functional and structural features of saposin-like proteins, Biochem. J. 389 (Pt 2) (2005) 249–257.
[8] R.S. Munford, P.O. Sheppard, P.J. O'Hara, Saposin-like proteins (SAPLIP) carry out diverse functions on a common backbone structure, J. Lipid Res. 36 (8) (1995) 1653–1663.
[9] E. Liepinsh, et al., Saposin fold revealed by the NMR structure of NK-lysin, Nat. Struct. Biol. 4 (10) (1997) 793–795.
[10] J. Kervinen, et al., Crystal structure of plant aspartic proteinase prophytepsin: inactivation and vacuolar targeting, EMBO J. 18 (14) (1999) 3947–3955.
[11] X. Qi, G.A. Grabowski, Differential membrane interactions of saposins A and C: implications for the functional specificity, J. Biol. Chem. 276 (29) (2001) 27010–27017.
[12] M. Rossmann, et al., Crystal structures of human saposins C and D: implications for lipid recognition and membrane interactions, Structure 16 (5) (2008) 809–817.
[13] A.M. Vaccaro, et al., Saposins and their interaction with lipids, Neurochem. Res. 24 (2) (1999) 307–314.
[14] C. Egas, et al., The saposin-like domain of the plant aspartic proteinase precursor is a potent inducer of vesicle leakage, J. Biol. Chem. 275 (49) (2000) 38190–38196.
[15] A. Ramamoorthy, et al., Cell selectivity correlates with membrane-specific interactions: a case study on the antimicrobial peptide G15 derived from granulysin, Biochim. Biophys. Acta 1758 (2) (2006) 154–163.
[16] H.L. Ziegler, T. Staalso, J.W. Jaroszewski, Loading of erythrocyte membrane with pentacyclic triterpenes inhibits Plasmodium falciparum invasion, Planta Med. 72 (7) (2006) 640–642.
[17] K.G. Payie, et al., Construction, expression and characterization of a chimaeric mammalian-plant aspartic proteinase, Biochem. J. 372 (Pt 3) (2003) 671–678.
[18] J.R. Mendieta, et al., Antimicrobial activity of potato aspartic proteases (StAPs) involves membrane permeabilization, Microbiology 152 (Pt 7) (2006) 2039–2047.
[19] M.G. Guevara, et al., Purification and properties of an aspartic protease from potato tuber that is inhibited by a basic chitinase, Physiol. Plant. 106 (1999) 164–169.
[20] M.G. Guevara, et al., Molecular cloning of a potato leaf cDNA encoding an aspartic protease (StAsp) and its expression after P. infestans infection, Plant Physiol. Biochem. 43 (2005) 882–889.
[21] J.R. Mendieta, et al., Cytotoxic effect of potato aspartic proteases (StAPs) on Jurkat T cells, Fitoterapia 81 (5) (2010) 329–335.
[22] M.G. Guevara, et al., An aspartic protease with antimicrobial activity is induced after infection and wounding in intercellular fluids of potato tubers, Eur. J. Plant Pathol. 108 (2002) 131–137.
[23] M.G. Guevara, et al., Potato aspartic proteases: induction, antimicrobial activity and substrate specificity, J. Plant Pathol. 86 (2004) 233–238.
[24] H. Bruhn, et al., Amoebapores and NK-lysin, members of a class of structurally distinct antimicrobial and cytolytic peptides from protozoa and mammals: a comparative functional analysis, Biochem. J. 375 (Pt 3) (2003) 737–744.
[25] P.K. Smith, et al., Measurement of protein using bicinchoninic acid, Anal. Biochem. 150 (1) (1985) 76–85.
[26] L.D. Mayer, M.J. Hope, P.R. Cullis, Vesicles of variable sizes produced by a rapid extrusion procedure, Biochim. Biophys. Acta 858 (1) (1986) 161–168.
[27] C.S.F. Böttcher, C.M. VanGent, C. Fries, A rapid and sensitive sub-micro phosphorus determination, Anal. Chim. Acta 1061 (1961) 203–204.
[28] J. Guillen, et al., Identification of the membrane-active regions of the severe acute respiratory syndrome coronavirus spike membrane glycoprotein using a 16/18-mer peptide scan: implications for the viral fusion mechanism, J. Virol. 79 (3) (2005) 1743–1752.
[29] J. Shin, P. Shum, D.H. Thompson, Acid-triggered release via dePEGylation of DOPE liposomes containing acid-labile vinyl ether PEG-lipids, J. Control. Release 91 (1–2) (2003) 187–200.
[30] A. Bernabeu, et al., Structure of the C-terminal domain of the pro-apoptotic protein Hrk and its interaction with model membranes, Biochim. Biophys. Acta 1768 (6) (2007) 1659–1670.
[31] M.R. Moreno, et al., Characterization of the interaction of two peptides from the N terminus of the NHR domain of HIV-1 gp41 with phospholipid membranes, Biochemistry 46 (37) (2007) 10572–10584.
[32] C. Perez-Iratxeta, M.A. Andrade-Navarro, K2D2: estimation of protein secondary structure from circular dichroism spectra, BMC Struct. Biol. 8 (2008) 25.
[33] J.R. Su, et al., Monomer–dimer transition of the conserved N-terminal domain of the mammalian peroxisomal matrix protein import receptor, Pex14p, Biochem. Biophys. Res. Commun. 394 (1) (2010) 217–221.
[34] B.R. Oakley, D.R. Kirsch, N.R. Morris, A simplified ultrasensitive silver stain for detecting proteins in polyacrylamide gels, Anal. Biochem. 105 (2) (1980) 361–363.
[35] F.G. Meng, et al., Dissociation and unfolding of GCN4 leucine zipper in the presence of sodium dodecyl sulfate, Biochimie 83 (10) (2001) 953–956.
[36] L. Zhong, W.C. Johnson Jr., Environment affects amino acid preference for secondary structure, Proc. Natl Acad. Sci. U. S. A 89 (10) (1992) 4462–4465.
[37] A. Jasanoff, A.R. Fersht, Quantitative determination of helical propensities from trifluoroethanol titration curves, Biochemistry 33 (8) (1994) 2129–2135.
[38] M. Tatti, et al., Structural and membrane-binding properties of saposin D, Eur. J. Biochem. 263 (2) (1999) 486–494.
[39] A.M. Vaccaro, et al., pH-dependent conformational properties of saposins and their interactions with phospholipid membranes, J. Biol. Chem. 270 (51) (1995) 30576–30580.
[40] R.I. Lehrer, T. Ganz, Antimicrobial peptides in mammalian and insect host defence, Curr. Opin. Immunol. 11 (1) (1999) 23–27.
[41] D. Gidalevitz, et al., Interaction of antimicrobial peptide protegrin with biomembranes, Proc. Natl Acad. Sci. U. S. A 100 (11) (2003) 6302–6307.
[42] R.P. Huijbregts, A.I. de Kroon, B. de Kruijff, Topology and transport of membrane lipids in bacteria, Biochim. Biophys. Acta 1469 (1) (2000) 43–61.
[43] K. Simons, E. Ikonen, Functional rafts in cell membranes, Nature 387 (6633) (1997) 569–572.
[44] K. Simons, W.L. Vaz, Model systems, lipid rafts, and cell membranes, Annu. Rev. Biophys. Biomol. Struct. 33 (2004) 269–295.
[45] J.P. Slotte, Sphingomyelin–cholesterol interactions in biological and model membranes, Chem. Phys. Lipids 102 (1–2) (1999) 13–27.
[46] A. Tannert, et al., Protein-mediated transbilayer movement of lipids in eukaryotes and prokaryotes: the relevance of ABC transporters, Int. J. Antimicrob. Agents 22 (3) (2003) 177–187.
[47] T. Abraham, et al., Isothermal titration calorimetry studies of the binding of the antimicrobial peptide gramicidin S to phospholipid bilayer membranes, Biochemistry 44 (33) (2005) 11279–11285.
[48] R.M. Verly, et al., Effect of cholesterol on the interaction of the amphibian antimicrobial peptide DD K with liposomes, Peptides 29 (1) (2008) 15–24.
[49] W.M. Yau, et al., The preference of tryptophan for membrane interfaces, Biochemistry 37 (42) (1998) 14713–14718.
[50] P. Jedlovsky, M. Mezei, Effect of cholesterol on the properties of phospholipid membranes.1. Structural features, J. Phys. Chem. B 107 (2003) 5311–5321.
[51] H. Khandelia, J.H. Ipsen, O.G. Mouritsen, The impact of peptides on lipid membranes, Biochim. Biophys. Acta 1778 (7–8) (2008) 1528–1536.
[52] H. Khandelia, Y.N. Kaznessis, Molecular dynamics investigation of the influence of anionic and zwitterionic interfaces on antimicrobial peptides' structure: implications for peptide toxicity and activity, Peptides 27 (6) (2006) 1192–1200.
[53] H. Khandelia, A.A. Langham, Y.N. Kaznessis, Driving engineering of novel antimicrobial peptides from simulations of peptide–micelle interactions, Biochim. Biophys. Acta 1758 (9) (2006) 1224–1234.
[54] V.C. Kalfa, et al., Congeners of SMAP29 kill ovine pathogens and induce ultrastructural damage in bacterial cells, Antimicrob. Agents Chemother. 45 (11) (2001) 3256–3261.
[55] C.E. Whitman, R.L. Travis, Phospholipid composition of a plasma membrane-enriched fraction from developing soybean roots, Plant Physiol. 79 (2) (1985) 494–498.
[56] R. Welti, et al., Profiling membrane lipids in plant stress responses. Role of phospholipase D alpha in freezing-induced lipid changes in Arabidopsis, J. Biol. Chem. 277 (35) (2002) 31994–32002.
[57] P. Runeberg-Roos, M. Saarma, Phytepsin, a barley vacuolar aspartic proteinase, is highly expressed during autolysis of developing tracheary elements and sieve cells, Plant J. 15 (1) (1998) 139–145.
[58] F. Chen, M.R. Foolad, Molecular organization of a gene in barley which encodes a protein similar to aspartic protease and its specific expression in nucellar cells during degeneration, Plant Mol. Biol. 35 (1997) 821–831.
[59] C. Faro, et al., Structural and functional aspects of cardosins, Adv. Exp. Med. Biol. 436 (1998) 423–433.
[60] C. Faro, et al., Cloning and characterization of cDNA encoding cardosin A, an RGD-containing plant aspartic proteinase, J. Biol. Chem. 274 (40) (1999) 28724–28729.
[61] K. Törmäkangas, et al., A vacuolar sorting domain may also influence the way in which proteins leave the endoplasmic reticulum, Plant Cell 13 (2001) 2021–2032.
[62] M. Vieira, et al., Molecular cloning and characterization of cDNA encoding cardosin B, an aspartic proteinase accumulating extracellularly in the transmitting tissue of Cynara cardunculus L, Plant Mol. Biol. 45 (5) (2001) 529–539.
[63] A. Schaller, C.A. Ryan, Molecular cloning of a tomato leaf cDNA encoding an aspartic protease, a systemic wound response protein, Plant Mol. Biol. 31 (5) (1996) 1073–1077.
[64] C.I. An, E. Fukusaki, A. Kobayashi, Aspartic proteinases are expressed in pitchers of the carnivorous plant Nepenthes alata Blanco, Planta 214 (5) (2002) 661–667.